Springer

Journal of Mechanical Science and Technology 23 (2009) 686~697

Journal of Mechanical Science and Technology

www.springerlink.com/content/1738-494x
DOI 10.1007/s12206-008-1217-8

Investigation on thermal characteristics of heat sinks for power module using STM †

Chung-Hyo Jung*, Young-Suk Chung and Hyung-Woo Lee

Samsung Electronics CO., LTD., 416, Maetan-3Dong, Yeongtong-Gu, Suwon-City, Korea

(Manuscript Received September 1, 2008; Revised December 7, 2008; Accepted December 20, 2008)

Abstract

The device that controls dynamic motions in a washing machine is called as MICOM. This device includes an IPM that controls the rotation of a tub. Also, the overheating of IPM gives cause for lowering the service life of an applied chip and is directly linked with its faults. A heat sink that is larger than the volume of the applied chip more than 50 times is installed to prevent such overheating. In the operation of the IPM, the temperature specification of the heat sink can be determined as 80℃ under the air temperature of 25℃. However, the heat sink used at the present time cannot satisfy this condition, so it is necessary to redesign such a heat sink to satisfy this condition. This study proposes an STM that is able to precisely calculate the temperature applied to IPM in a system level prior to redesigning the heat sink. The STM can be considered as a model that complements a JEDEC analysis model. This model implements a parameter analysis to perform the optimization of a heat sink and verifies the priority of parameters to reduce material costs. Furthermore, it investigates a counterproposal that replaces the conventional cooling methods in which it seeks a counterproposal that performs heat dissipation in a device according to the SoC of chips and is able to suppress EMI.

Keywords: CFD; Heat sink; IPM(intelligent power module); JEDEC(joint electron device engineering council); PBA(printed board assembly); STM(system-level thermal model); Washing machine

1. Introduction

The devices that controls the dynamic motions in a washing machine is known as a control unit. The control unit is determined as a printed board assembly (PBA) unit in which the chip, which controls rotational motion, is an intelligent power module (IPM). A tub performs both forward and reverse rotations repeatedly and that applies overloads to the control element. Thus, the IPM generates excessive heat while a washing machine is being operated. Such overheats in the IPM may be directly connected to the decrease in the service life of chips and malfunction of the machine. Also, the excessive heat is directly connected to the environment where the machine is operated. In general, washing machines are used in closed, high-temperature, and high-humidity environments. Moreover, the PBA is wrapped by waterproof rubber and cover-PCB and that represents difficulties in the dissipation of such heat to the outside easily. A thermal design is required to perform the function of the IPM in these poor surroundings. Expenses on such a design have rarely been paid until recent years. The existing optimum heat sink design has been conducted in a single product level [1-6]. Also, there are some programs of such optimum heat sink design for the person who did not major in heat transfer [7]. However, there are no studies that investigate the analysis of heat generation in chips and the optimum design of heat sinks simultaneously in heat sink installed environments. Thus, this study attempts to apply a system-level thermal management (STM) method [8] used in the thermal design of processors for LCD-TVs to the optimum design of the heat sink

† This paper was recommended for publication in revised form by Associate Editor Jae Dong Chung

* Corresponding author. Tel.: +82 31 277 7178, Fax.: +82 31 277 7731
E-mail address: jungchunghyo75@hanmail.net

of the IPM for washing machines.

IPMs used at the present time represent a problem in overheating. Although heat sinks are used to prevent such overheat, they exceed the specific temperature of 80℃. Thus, the on/off time that controls a motor should be configured as a short interval. Otherwise, the IPM will cause troubles due to overheating. It is necessary to establish a cooling method that satisfies the temperature specification of heat sinks without applying such a short interval for motor controls.

The thermal analysis of the IPM using CFD can be classified as three different levels. First, at a package level, the temperature of chips can be evaluated by using a JEDEC model that is a standard verification environment. Also, the cooling level of chips can be verified by installing heat sinks used in actual products. Second, at the PCB level the heat transfer in chips can be observed. It is possible to verify not only how the heat of the package is transferred to the board but the relation to neighboring heating elements. Third, at the system level, it can analyze the temperature of chips (T_j) according to the operation mode of a washing machine. Because the temperature of chips can be determined in a system environment eventually, a highly reliable analysis model is actually required. Therefore, the IPM temperature measured during the operation of a washing machine will be applied to analysis of the system and verify the correlation of the system. Here, parameter estimation is also performed to well match the analysis results to the experimental results. Then, a validated model (STM) can be established through this process. This model is used to investigate various environments where the IPM is operated, and optimization of heat sinks, and other cooling methods.

The objective of this study can be classified as two ideas. First, this study configures a cooling goal that satisfies the temperature specification by investigating the present heat generation level of the IPM. Second, this study establishes an STM (system-level thermal model) based on the data produced in experiments. This model can be used to optimize heat sinks that satisfy such temperature specification.

2. Analysis and experiment

2.1 Establishing a JEDEC analysis model

In general, it has been known that an increase in the junction temperature (T_j) of a device by 10℃ decreases its service life as a half level and increases trouble rates more than double. In the case of power devices, the thermal design of the T_j can be determined as an 80% level of the maximum allowable temperature specified in a design manual. The satisfaction of this specification can be verified by thermal resistances. The thermal resistance [9, 10] can be defined as the convection and conduction environments of chips. The value of T_j can be estimated by using Eq. (1) in a convection environment. Here, the thermal resistance expressed by ψ is called as a thermal characterization parameter.

$$\Psi_{jt} = \frac{T_j - T_t}{P_d} \tag{1}$$

Eq. (1) can be expressed by an identical equation. Where, the value of ψ_{jt}^* is about 1.0.

$$T_j - T_t = \Psi_{jt}^* p_d \tag{2}$$

Then, the thermal resistance between the temperature (T_j) of the die and the temperature (T_a) of atmosphere can be determined as noted in Eq. (3).

$$R_{ja} = \Psi_{jt} + \Psi_{ta} \tag{3}$$

Also, the thermal resistance can be defined as Eq. (4) as the value of T_j is produced by Eq. (1) or measured by using an equipment.

$$\theta_{ja} = \frac{T_j - T_a}{P_d} \tag{4}$$

Next, the heat that can only be transferred by conduction can be described as follows. If most of the heat generated in the die is conducted to the lower board, it can be defined by Eq. (5).

$$\theta_{jb} = \frac{T_j - T_b}{P_d} \tag{5}$$

In addition, if most of the heat generated in the die is conducted to the heat sink installed at the upper section of the package, it can be defined by Eq. (6).

$$\theta_{jc} = \frac{T_j - T_c}{P_d} \tag{6}$$

The thermal resistance is used for presenting the package to a thermal network [11]. In general, it is referred to as a compact thermal model. However, a detailed thermal model uses 100% of the ECAD of the package. It is also called a compact model that simply produces a model by considering the thermal conduction of the package.

Fig. 1 illustrates the IPM manufactured by Mitsubishi and the cross-section of a typical IGBT. This chip is an inverter device to control motors and that includes six chips of the fifth generation PLANA IGBT (insulated gate bipolar transistor). The rating voltage and current of this chip are 600 V and 15 A, respectively. Also, its length, width, and thickness are 38 mm, 24 mm, and 3.5 mm, respectively.

The JEDEC strictly controls the test environment of chips by the rule of "JEDEC Standard JESD51-2" [12]. Because the fabrication of the sample for measuring the T_j of the IPM requires considerable expense, the temperature is calculated in a virtual test chamber as shown in Fig. 3. To perform this calculation, it is necessary to produce a compact model of the IPM. The compact model presented Fig. 2 can be used to perform an analysis in a chamber environment as shown in Fig. 3. Then, the thermal characteristic value can be obtained for calculating such thermal resistance.

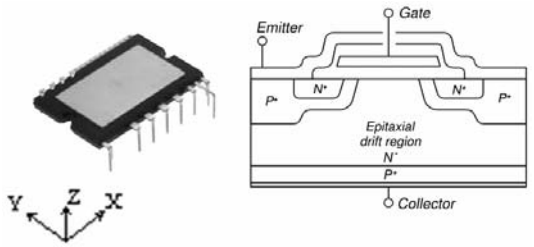

Fig. 1. Outward appearance of the IPM and a circuit.

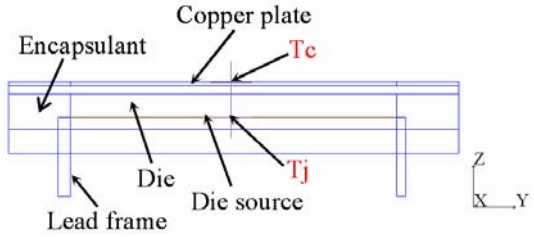

Fig. 2. Compact model of the IPM.

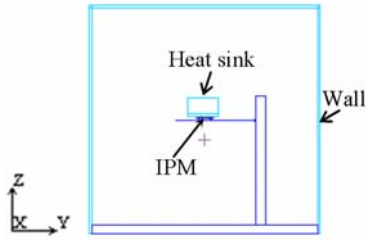

Fig. 3. Simulation model of the JEDEC standard.

A numerical simulation was performed using a Flotherm V6.1 s/w. In the calculation, the conditions of the external atmosphere were configured as 25℃ and 1 atm. In the calculation of velocity fields (automatic algebraic), conditions of laminar/turbulent flows are to be configured. Also, in the calculation of temperature fields, conditions of convection, conduction, and radiation are to be determined. In addition, the number of convergences in flow, temperature, and pressure is to be configured as 5, 300, and 50, respectively, for the calculation.

Fig. 4 shows the obtained IPM temperature by using a JEDEC analysis model. It can be seen that the value of T_j (for 20 W) decreased about 79.9℃ (Δ T) as a heat sink is installed on the IPM. Table 1 shows

Table 1. Temperature and thermal resistance of the chip (without a heat sink).

Power (W)	P_d	20.0
Temperature (°C)	T_j	190.72
	T_t	186.99
	T_a	25.0
R_{th} (°C/W)	θ_{ja}	8.286
	ψ_{jt}	0.1865

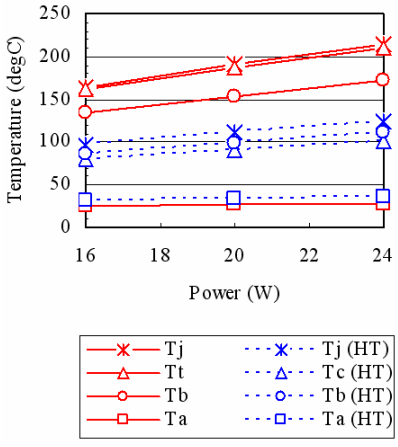

Fig. 4. Temperature comparison according to the presence of a heat sink (T_j(*HT*):temperature in using the heat sink).

the thermal characteristics as a heat sink is not installed on the IPM. In Table 1, the value of T_t shows the temperature of the top surface of the package.

2.2 Design of heat sinks

As shown in Table 1, the value of T_j exceeds the allowable temperature range as a heat sink is not installed. The chip that generates high heat will be destroyed due to thermal runway. To prevent such trouble, a heat sink is to be installed the chip.

Fig. 5 shows a rectangular fin [13, 14] in a heat sink. The general equation for calculating the surface area of a fin can be expressed as Eq. (7).

$$A_t = NA_f + A_b \tag{7}$$

where A_f and A_b represent the areas of a fin and the base, respectively.

The factor for calculating the efficiency of a rectangular fin can be obtained by using Eq. (8). Also, the value of η_f (fin efficiency) that corresponds to the obtained value can be produced from Fig. 6.

$$L_c^{3/2}\left(\frac{h}{\kappa A_m}\right)^{1/2} \tag{8}$$

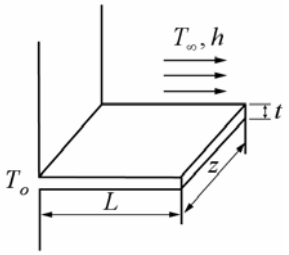

Fig. 5. Longitudinal fin with a rectangular profile.

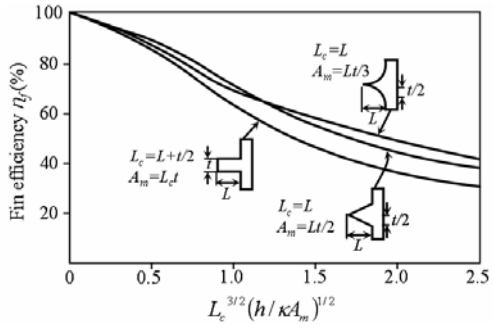

Fig. 6. Efficiency of rectangular fins [14].

The total efficiency of a heat sink, which uses N fins, can be obtained by using Eq. (9).

$$n_t = 1 - \frac{NA_f}{A}\left(1 - n_f\right) \tag{9}$$

Also, the heat flow of a heat sink in a one-dimensional steady-state can be obtained by Eq. (10).

$$q_t = n_t A_t h \Delta T \tag{10}$$

However, the following assumptions are required to use this equation:

(1) Heat is only transferred by one-dimensional conduction.
(2) Material properties are constant.
(3) Radiation heat exchanges with neighboring elements are neglected.
(4) The convection heat transfer factor (h) is constant.
(5) Contact thermal resistance with the heat sink is neglected.

A one-dimensional design of a heat sink can be performed by using Eqs. (7-10). The thermal design of the heat sink can be verified by a one-dimensional calculation. Table 2 shows the parameters used in the one-dimensional design of a heat sink. The calculation is applied to the present design specification, Type 1, and Type 2. The present design specification shows the parameter of the heat sink used in the completed products forwarded to markets. The Type 1 and Type 2 are proposed based on this specification. The Type 1 increases the height of the heat sink compared to the present product and number of fins. Also,

Table 2. Parameters used in the calculation.

Item		Present	Type 1	Type 2
Fin	L (mm)	20	40	55
	W (mm)	40	40	40
	t (mm)	3.5	3.5	3.5
	N	11	18	13
Fin area (m^2)		0.02178	0.06276	0.06166
Fin efficiency		0.96	0.96	0.96
k (W/mK)		186	186	186
h (W/m^2K)		10	10	10
T_a (°C)		25	25	25
Tmax of fin (°C)		75	60	60
Heat flow (W)		10.60	21.12	20.75

the Type 2 increases the height of the heat sink and two fins only. The heat flow for each type can be obtained by substituting the parameters noted in Table 2 to Eq. (10).

As a result, the heat flow of the present model was 10.60 W, and the Type 1 and Type 2 showed 21.12 W and 20.75 W, respectively. It is evident that it is not sufficient to fully dissipate heats using the present specification as the heat flow is 20 W. Based on the investigation, it is possible to propose a heat sink shape that satisfies the target temperature of the fin.

2.3 System-level experiment and analysis

A device that controls dynamic motions of a washing machine is a printed board assembly (PBA). In the aspect of material expenses, the PBA is the top third part in a washing machine assembly. Also, single power, low price, and high speed technologies are required to reduce development costs. To achieve a cost reduction, reductions in the PCB area, PBA standardization, reduction in the number of circuit parts by SoC, and development of high efficiency IPMs are the most urgent necessity. In particular, the IPM investigated in this study needs to develop technology that reduces current losses through improvements in switching characteristics and IGBT structures.

A washing machine can be classified according to capacity, such as ultra large scale, large scale, and automatic machine. Also, the PBAs applied to these models are differently classified. This study performed a thermal analysis of the PBA used in an ultra large machine. Fig. 7 (a) shows an image of the PBA. The IPM is located at the lower center under the heat sink. The IPM plays a role in the control of the power applied to the motor. In the washing process, the IPM generates heat about 20 W. If the heat is not effectively dissipated, the PCB will be in thermal trouble due to such high heat. To avoid this problem, a forced on/off time is configured to control the motor. However, it causes a lowering in the performance according to the increase in the cycle of control. Thus, it is necessary to perform a design in heat sinks through a precise temperature estimation of the IPM.

Meanwhile, a ZIG (MICOM) was fabricated to measure the temperature of the IPM in an operation process. This device controls the power applied to the IPM in order to reproduce a condition in which a washing machine is continuously operated. The temperature of the heat sink installed in the washing machine with the ZIG is to be measured in a temperature/humidity chamber (DS-133MTHP, MIMOS Tech., 2004). Fig. 8 shows the temperature of the heat sink according to the change in the air temperature of the chamber where *dT* represents the subtraction of the operation temperature of the chamber from the temperature of the heat sink. If the temperature of the chamber is increased, the time in which the temperature of the heat sink approaches to a steady-state is delayed. The average temperature and standard deviation of the heat sink for three operation conditions after 80 minutes from the operation were 52.28℃ (0.71), 52.54℃ (0.83), and 52.68℃ (0.52), respectively.

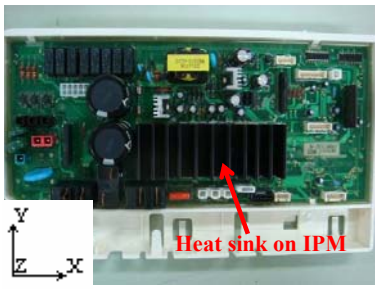

(a) PBA

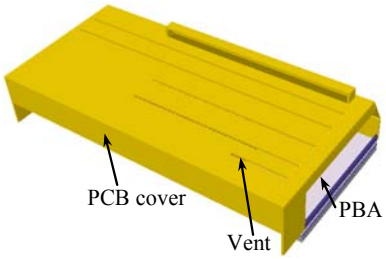

(b) Simulation model

Fig. 7. PBA used in a Washing Machine.

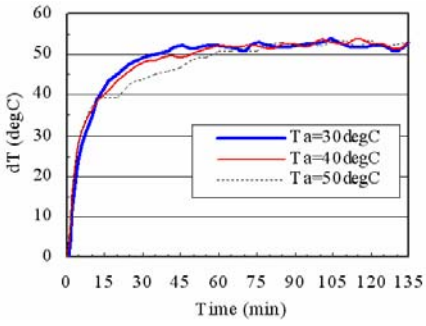

Fig. 8. Heat sink temperature according to the temperature of the chamber.

Based on the reliability guaranteed in this experiment, the experiment can be classified in two ways according to the existence of a waterproof case (PCB cover) installed on the PBA. In addition, a mock-up was fabricated to measure the temperature according to the type of heat sink. Table 3 shows such temperatures of the Type 1 and Type 2. First, in the temperature of the present type of heat sink, it increases up to 83.3℃ (without a PCB cover) maximum, which means that the temperature exceeds the specification of 80℃. However, in the case of the proposed heat sink, which is applied to improve such a problem, the maximum temperature, such as 71.0℃ (without a PCB cover), fully satisfies the specification. Based on this analysis, it is considered that the present specification can be replaced by Type 1 and Type 2. However, in the case of Type 2, although it shows better thermal characteristics than that of Type 1, it represents a 10 mm of interference with the cover in the PCB assembly process. Also, the IPM can be significantly affected by external shocks in a drop test for parts due to the contact of the heat sink. Thus, Type 1 is a better way than Type 2.

In addition, there is a difference in the temperature between the inside temperature (*Ta*-S) and the outside temperature (*Ta*-R) of about 10℃ according to the condition presented in Table 3. Although the temperature between the inside and the outside showed a difference of about 10℃, the temperature of the heat sink represented around 4℃ with or without a PCB cover. It shows that it is not an effective way for cooling the heat sink even though several vents are installed on a PCB cover. Therefore, the best way to cool the IPM is to change the size of the heat sink.

2.4 Establishing an STM (System-level Thermal Model)

This section attempts to determine the final design specification of the heat sink based on the results investigated in the previous section including the establishment of a system-level thermal model (STM) based on the results of the experiment. The temperature data used in this section uses the data obtained in the temperature chamber. In addition, the reference temperature (T_a) used in the analysis uses the inside temperature of the washing machine set. The inside temperature (*Ta*_S) of the set noted in Table 3 shows about 10℃ higher than that of the configured temperature of the chamber. Also, there exists a proportional relationship between the inside temperature of the set (temperature around the PCB) and the temperature of the fin (Fig. 9). It can be determined regardless of the shape and size of the heat sink.

The heat sink of the Type 1 presented in Table 2 was changed to the specification of the item of "Modify" presented in Table 4 in which the length of the heat sink was extended by 15 mm, the thickness was reduced by 1/2, and the number of fins increased by 8 in order to improve heat dissipation effects. In the case of the use of the Type 1, the temperature of the fin was 75.6℃ (at T_a=38.5℃). However, the Modify Type was measured by 76.7℃ (at T_a=42.0℃). Thus, the heat sink specified under Modify showed a better cooling result than the Type 1 about 2.4℃, and it showed about 16℃ lower level than the present design specification. Although it represents such improved cooling effects, it has some disadvantages,

Table 3. Bottom temperature of the heat sink for the use of a PCB cover.

Item	Present Type		Type 1		Type 2	
PCB cover	No	Use	No	Use	No	Use
Tmax (°C)	83.3	86.7	71.0	75.6	66.8	70.2
T_a_S (°C)	37.1	35.7	35.8	38.5	37.4	36.1
T_a_R (°C)	26.0	25.6	25.5	28.0	25.7	24.5
-	T_a_S : Inside temperature of the set T_a_R : Room Temperature					

Table 4. Improvement of the heat sink (bottom temperature).

Item	Present	Modify
Length (mm)	110	125
Height (mm)	20	40
W (mm)	40	40
t (mm)	3(upper), 4(lower)	Experiment/analysis (upper 1.7, lower 2.5)
Base (mm)	4	4.5
Number of fins (*N*)	11(including left and right)	19(including left and right)
Pitch (mm) between fins	5-6	3.4-4.1
Fin area (m^2)	0.02178	0.065772
Weight (*g*)	132	250
Price (₩)	600	1100
Tmax (°C)	93.6	76.7
T_a (°C)_Set inside	42.9	42.0

such as increases in weight and cost. In spite of these disadvantages, it is necessary to reflect the specification of Modify in order to prevent failures in the PCB.

Fig. 9 illustrates the comparison of the analysis data obtained by using the STM and the experiment results. The STM is able to precisely calculate the values of T_j and T_c in the chip in an operation condition of the set. The establishing process of the STM can be described as follows. First, a test is to be applied by using an experimental DOE. The, analysis parameters are to be configured to build an analysis model in which the X's factor and boundary condition are to be extracted to satisfy the target value of Y's.

Next, it is necessary to verify whether the established model satisfies the results of the experiment according to the various environmental conditions and power of the chip. Based on the verification, the STM can be established. It is evident that the temperature of the fin obtained by using this model shows good agreement with the results of the experiment as illustrated in Fig. 9. Also, the temperature of the fin increased linearly according to the increase in the inside temperature of the set (T_a).

In addition, the value of T_c was measured for the condition without installing a heat sink on the IPM. Although it was difficult to measure the accurate value during the operation due to the failure of the chip caused by overheat, it was estimated to be around 200℃. The STM was established by considering this value and the temperature of the fin obtained under the condition with installing a heat sink. In that process, the temperature of the fin and the value of T_c were configured as the values that approached the experimental values at the same time. Thus, it was possible to analytically determine the value of T_j which is difficult to easily produce in an ordinary way. Table 5 shows the comparison between the values obtained from the JEDEC analysis model for T_j, and T_c, and R_{th} and using the STM. As shown in Table 5, the value of T_j obtained with the JEDEC model represented a 10.9℃ higher level than that of the STM.

As mentioned above, the thermal property of the chip obtained by using the JEDEC analysis model showed large differences compared with that of the operation condition (or of using the STM). Therefore, it can be considered that the STM model provides a more precise way to design heat sinks. Thus, it was necessary to establish the STM due to such applicability. Fig. 10 shows the results of the calculation of temperature by using the STM for the heat sink de-

Table 5. Temperature and thermal resistance of the chip (with a heat sink).

Model	Temperature (°C)		R_{th} (°C/W)
	T_j	T_c	θ_{jc}
JEDEC	110.85	90.15	1.035
STM	99.99	80.72	0.9635

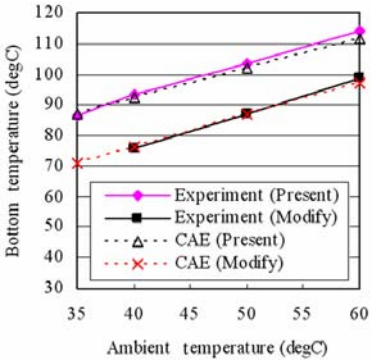

Fig. 9. Bottom temperature of the heat sink according to changes in air temperature.

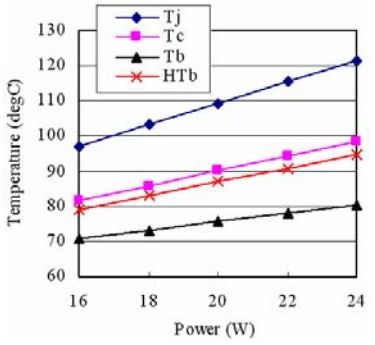

Fig. 10. Temperature of the present design specification (T_a=35℃).

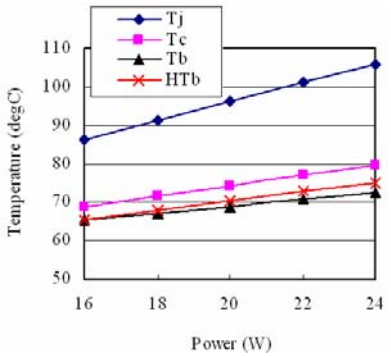

Fig. 11. Temperatures in the modified specification (T_a= 35℃).

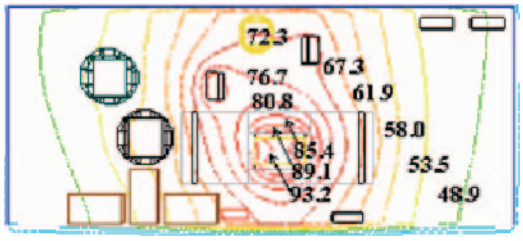

Fig. 12. Isotherm curves of the PCB surface in the present design specification (T_a=35℃).

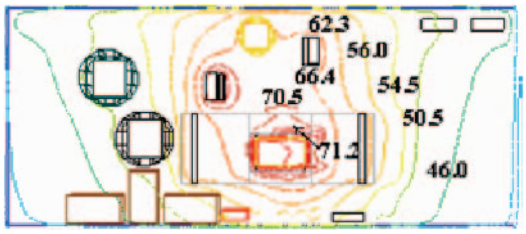

Fig. 13. Isotherm curves of the PCB surface in the proposed design specification (T_a=35℃).

signed by the present specification.

Also, Fig. 11 shows the thermal property calculated by the new specification, which is modified from the present specification, as noted in Modify. In Fig. 10 and Fig.13, although the values of T_c and *HTb* (bottom section temperature of the heat sink) show a decrease in T_j as a linear manner, the value of in Fig. 11 shows a relatively small decrease. First, it was due to the fact that the thermal resistance between the IPM and the board represented larger values than the values between the IPM and the heat sink. It showed no significant decreases in the temperature of T_b. Therefore, it is necessary to increase the dissipation of the heat of the chip toward to the inside of the board by reducing the thermal resistance between the IPM and the board.

Second, because the heat dissipated to the heat sink showed a large amount of it, the values of T_j and T_c decreased by 15-18℃ maximum. However, the value of T_b decreased by 8℃ only (IPM=24 W). Thus, the lowering effect of T_b in the bottom section of the IPM showed a low level relatively.

Fig. 12 and Fig. 13 show the isotherm curves in which the heats generated from the IPM and the neighboring elements, such as diodes and transformer, represented a thermal equilibrium on the surface of the PCB.

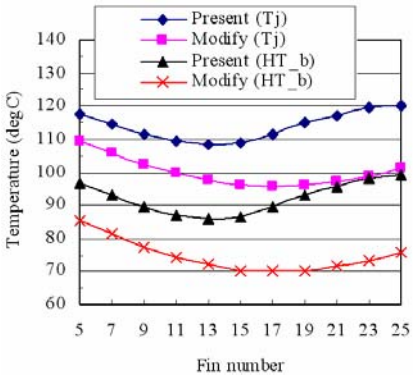

Fig. 14. Temperature determined by the number of fins (T_a=35℃).

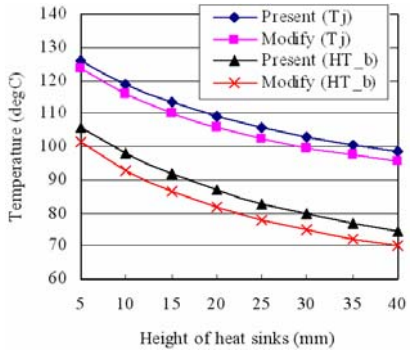

Fig. 15. Temperature determined by the height of the heat sink (T_a=35℃).

3. Optimization and cooling plans for heat sinks

3.1 Optimization of new heat sinks

Fig. 14 represents the results of the thermal analysis by configuring the number of fins as a parameter among the design parameters of the heat sink. As shown in Fig. 14, the number of fins applied in the present design specification was 13 in which the values of T_j and *HTb* (bottom section temperature of the heat sink) were minimized by such numbers of fins. However, the present design specification shows 11 fins and that requires two more fins (see Table 4). In addition, although the number of fins determined in Modify will be extended as 19, it is configured to be 17 as the optimum number [15] of fins as illustrated in Fig. 14. Regarding the change in the values of Present (T_j) and Modify (T_j) according to the increase in the number of fins, the former shows the maximum temperature (120℃) for 25 fins, which shows a smaller number of fins compared to that of the latter.

Table 6. Optimum number of fins according to the size of the heat sink (Fixed height: 20 mm, T_a=35℃).

Fin type		65 mm	80 mm	95 mm	110 mm	125 mm
Top with:3.0 mm Base with:4.0 mm	Fin number	8	10	11	13	15
	T_j	118.3	114.2	111.7	108.4	108.0
	HTb	97.7	92.6	89.1	85.9	83.8
Top with:1.7 mm Base with:2.5 mm	Fin number	10	12	15	15	17
	T_j	116.1	112.3	109.3	106.7	106.6
	HTb	95.2	90.5	87.0	84.0	82.4

If the total thickness of the fin exceeds the value of 100 mm (25 fins*4 mm (thickness)), the cooling effect will not be presented as the length of the heat sink is determined by 110 mm. However, in the case of the specification determined in Modify, the cooling effect will be presented if the number of fins (2.5 mm thickness) is configured as more than 25. It is evident that the thinner fins represent a greater cooling effect for the same size of the heat sink as described above.

Fig. 15 illustrates the results of the calculation by applying the height of the heat sink only as a parameter. The maximum allowable height of the heat sink is 44mm (a vertical height from the top surface of the IPM to the PCB cover). By considering this height, the height of the heat sink was determined as 5~40 mm. As shown in Fig. 15, the temperature decreases according to the increase in the height of the heat sink. Based on this characteristic, the heat sink designed as a shape that shows a longer length in a vertical direction than that of a horizontal direction will present advantages for such thermal properties.

Table 6 shows the length of the heat sink, number of fins, and lowest temperature produced according to fin type. However, the height of the heat sink was fixed by 20 mm. As shown in Table 6, it is possible to verify the optimal number of fins according to the length of the heat sink. Also, the thinner fin shows a lower temperature in which the difference is about 2℃. In the calculation conditions noted in Table 6, the temperature will be determined in a linear way if the height of the heat sink is configured as a high value (see Fig. 15). Similarly, the height of the heat sink in which it is applied as a parameter shows an advantage in heat dissipation compared to that of the parameter determined by the length of the heat sink. Thus, it is necessary to first consider the height of the heat sink. Meanwhile, in terms of the determination of the parameters defined in the design specification of Modify (Table 4), it presents some advantages in cost reduction for the configuration of the length and height of the heat sink in which the length needs to be fixed by 110 mm, and the height needs to be configured from 20 mm to 40 mm. The design of the heat sink based on these facts will satisfy both temperature and cost sides.

3.2 Cooling plan

The cooling plan [16] of the IPM is considered as two concepts: material costs and thermal performance. Also, a method that reduces the dissipation of EMI caused by the SoC (system on chip) is to be regarded.

Although the specification of Modify presented in Table 4 shows very excellent performance (cooling it as -16℃) compared to the present design specification, it shows an increase in material cost of about 1.8 times. As shown in Fig. 15, however, the cooling shows a decrease in the temperature of the fin as 11℃, the material cost will increase about 1.4 times as the length of the heat sink is fixed in the present design specification, and the height is configured by 40 mm higher than the present size. Here, it will be possible more likely to decrease the temperature if the optimal number of fins is determined based on the graph illustrated in Fig. 14. The best way to satisfy the needs of both material costs and thermal performances, however, is by developing design technology of low power consumption IPMs. If it is possible, the value of T_j will decrease by 3℃ as the power consumption of the IPM decreases by 1W, as shown in Fig. 10.

Meanwhile, we propose a cooling plan for the fin through applying various methods as follows:

(a) Changing the contact section between the IPM and the PCB which is a type of rubber (k=0.3 W/mK) to a thermal pad (k=1.5 W/mK).
(b) Connecting the length of the fin of the heat sink that is to be elongated to the PCB cover directly.
(c) Changing the package type of the IPM from DIP (dual inline PKG) to BGA (ball grid array).

Table 7. Thermal characteristics for the use of an EMI Shield (T_a=35℃).

-	T_j	T_c	*HTb*	T_a
Present (℃)	109.31	90.05	87.03	35.0
Using EMI Shield (℃)	98.58	78.80	75.57	35.0

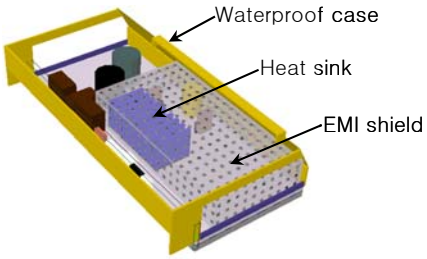

Fig. 16. Installation of an EMI Shield.

(d) Installing 416 via holes on the board that is contacted to the IPM during the consideration of (c).

(e) The allowance of EMI may exceed the allowable level due to the highly integrated parts used in the circuit. To prevent this problem, an EMI shield can be used as shown in Fig. 16.

Based on these five suggestions, the following conclusions are drawn:

There were no cooling effects on the chip for the application of (a). In the case of the idea of (b), the chip may present some shocks even though the value of T_j decreased by 14.5℃. Also, the suggestion of (c) represented no specific cooling effects on the chip. For the application of (d), the value of T_j decreased by 1.5℃. Finally, in the suggestion of (e), the value of T_j decreased by 10℃ as presented in Table 7. As a result, although the idea of (e) improves thermal properties and suppresses the dissipation of EMI, it significantly increases material costs. Thus, it is necessary to develop a low power consumption technology of IPMs and perform an optimum design of circuit boards in order to compensate for this problem [17, 18].

4. Conclusions

The IPM controls the rotational motion of the tub in a washing machine. A heat sink is installed on the IPM to prevent overheat during its operation. In the design process of heat sinks, the performance and heat dissipation performance are simultaneously considered. Satisfying such conditions requires an optimization of the heat sink. This study developed the STM in order to precisely determine the temperature of the IPM. This model can be used to estimate the temperature of the IPM and perform an optimized design of a heat sink. The conclusions obtained from this study can be summarized as follows:

(1) The environment for evaluating the thermal performance of the chip is ruled by the JEDEC 51-2. This study applied a virtual analysis environment that corresponds to the rule, and the virtual environment is called the JEDEC analysis model. The thermal property of the heat sink applied in this study was analyzed in detail with this model. In addition, the thermal property of the IPM was evaluated by installing the heat sink used in the present set to the IPM.

(2) The temperature specification of the heat sink for IPMs was specified by 80℃ (T_a=25℃). However, the present design specification does not satisfy this specification. Thus, this study applied a one-dimensional design theory for obtaining this condition. As a result, this study has drawn a design parameter that decreases the temperature of 15℃ compared to that of the present design specification. Regarding the verification of the parameter, a mock-up was fabricated and that satisfied the value presented in the theory.

(3) The thermal property obtained by using the JEDEC analysis model represented large differences in temperature compared to that of the measured value in an actual set environment. To identify such differences, the STM was established through an experiment. The value of T_j produced by using the JEDEC showed about 10.9℃ higher than that of the STM. It is evident that the thermal evaluation of the chip used in a set environment is the way of STM more effective than that of the JEDEC.

(4) The STM was applied to perform the optimization of the heat sink. This study determined the optimum number of fins according to the length of the heat sink for two different types of fins. Here, one point to remember is that if the height of the heat sink is fixed and the length of the heat sink is elongated from 110 mm (the present design) to 125 mm (the specification defined in Modify), the temperature of the fin is only decreased by 2℃. It means that the cool-

ing effect is very small in accordance with the increase in material costs. Thus, the number of fins and height of the heat sink are first considered in the optimization of the heat sink.

(5) Five cooling methods were proposed to improve the cooling effect of the IPM. As a result, there were alternative methods that decrease material costs and improve the cooling effect. However, a suggestion that controls the EMI generated by the SoC for the parts used in circuits was effective. It will present excellent effects in heat dissipation and EMI shield even though it causes an increase in material costs.

Nomenclature

A : Total heat-transfer area, including fins and exposed tube or other surfaces fin length(m)
A_b : Areas of the base (m^2)
A_f : Surface area of a fin (m^2)
A_m : Fin profile area (m^2)
h : Heat-transfer coefficient (W/m^2K)
L_c : Fin length (m)
n_t : Total efficiency
P_d : Total power (heat) dissipated in a chip (W)
T_a : Ambient temperature (℃)
T_b : Temperature measured on or near the component lead (℃)
T_c : Package (top surface) temperature (℃)
T_j : Junction temperature at a steady-state (℃)
T_t : Package (top surface) temperature at a steady-state measured using thermocouples (℃)

Greek symbols

ψ_{jt} : Junction-to-top thermal characterization parameter (℃/W)
θ_{ja} : Thermal resistance from the junction-to-ambient (℃/W)
κ : Thermal conductivity (W/mK)

References

[1] S. Krishnamoorthi, K. Y. Goh, Desmond Y. R. Chong, R. Kapoor and Anthony Y. S. Sun, Thermal characterization of a thermally enhanced QFN package, *2003 Electronics Packaging Technology Conference*, (2003).

[2] D. J. Kim and S. J. Kim, Compact modeling of fluid flow and heat transfer in straight fin heat sinks, *ASME Journal of Electronic Packing*, 126 (2004) 247-255.

[3] J. Richard Culham and Yuri S. Muzychka, Optimization of plate fin heat sinks using entropy generation minimization, *IEEE Transactions on Components and Packaging Technologies*, 24 (2) (2001) 159-165.

[4] K. W. Park, P. K. Oh and H. J. Lim, Optimum design of a pin-fins type heat sink using the CFD and mathematical optimization, *International Journal of Air-Conditioning and Refrigeration*, 13 (2) (2005) 71-82.

[5] K. J. Riu, C. W. Park, C. S. Jang and H. W. Kim, Cooling characteristics of wing fin heat sink, *Korean Journal of Air-conditioning and refrigeration Engineering*, (In Korean), 16 (8) (2004) 728-740.

[6] J. H. Kim, J. H. Yun, O. K. Kwon and C. S. Lee, An experimental study on the thermal resistance characteristics of layered heat sink, *Korean Journal of Air-conditioning and refrigeration Engineering*, (In Korean), 13 (4) (2001) 271~279.

[7] http://www.ates.co.kr/, qfin 3.1 S/W.

[8] E. S. Cho, M. N. choi, C. H. Jung, et. al., Set-level thermal management with package thermal design in digital TV application, *11th ITherm Conference*, Orlando, Florida, USA. (2008) 598-603.

[9] S. Y. Kim and R. L. Webb, Analysis of convective thermal resistance in ducted fan-heat sinks, *IEEE Transactions on Components and Packaging Technologies*, 29 (3) (2006) 439-447.

[10] Z. Duan and Y. S. Muzychka, Impingement air cooled plate fin heat sinks part II-thermal resistance model, *2004 Inter Society Conference on Thermal Phenomena*, (2004) 436-443.

[11] A. Nakata, S. Tanaka, K. Sugano, T. Tsuchiya and O. Tabata, Electrical equivalent circuit model of microfluidic system containing piezoelectric valveless micropump and viscoelastic PDMS microchannel, *Mechanical Engineering Congress*, (In Japanese), Japan(MEC J-08), 8 (2008) 23-24.

[12] EIA/JESD51-2, Integrated circuits thermal test method environment conditions-natural convection (still air), (1995).

[13] J. R. Culham, M. M. Yovanovich and S. Lee, Thermal modeling of isothermal cuboids and rectangular heat sinks cooled by natural convection, *IEEE Transactions on Components, Packaging, and Manufacturing Technology-part A*, 18 (3) (1995) 559-566.

[14] J. P. Holman, Heat transfer 7th edition in SI units,

McGraw-Hill Book Company, McGraw-Hill International, UK, (1992) 42-65.

[15] H. Shaukatullab, W. R. Storr, B. J. Hansen and M. A. Gaynes, Design and optimization of pin fin heat sinks for low velocity applications, *Twelfth IEEE SEMI-THERM™ Symposium*, Austin, TX, USA. (1996) 151-163.

[16] C. J. Shih and G. C. Liu, Optimal design methodology of plate-fin heat sinks for electronic cooling using entropy generation strategy, *IEEE Transactions on Components and Packaging Technologies*, 27 (3) (2004) 551-559.

[17] T. Y. Wang and C. C. P. Chen, SPICE-compatible thermal with lumped circuit modeling for thermal reliability analysis based on modeling order reduction, *IEEE Computer Society*, (2004).

[18] Y. Joshi, M. Baelmans, D. Copeland, C. J. M. Lasance, J. Parry and J. Rantala, Challenges in thermal modeling of electronics at the system level, *IEEE Transactions on Components and Packaging Technologies*, 24 (4) (2001) 611-613.

Chung-Hyo Jung acquired the doctoral degree in the Dept. of Science for Open and Enviromental Systems at Keio University in 2003. The specialty in the doctoral course was GSMAC-FEM and studied on MHD (magnetohydrodynamics). Dr. Jung joined Samsung Electronics Co., Ltd. as a CFD engineer in 2003. Also, he has worked at Samsung Advanced Institute of Technology and has charged in the thermal analysis of semi-conductors (system LSI). One of the Dr. Jung's major concerning fields is the mechanical application of Lie-Groups.